Developmental transcriptomic profiling of non-sensory vestibular epithelium reveals ionic contribution to endolymph formation

Sang Hyun Kwak

Department of Medicine
The Graduate School, Yonsei University

Developmental transcriptomic profiling of non-sensory vestibular epithelium reveals ionic contribution to endolymph formation

Directed by Professor Sung Huhn Kim

The Doctoral Dissertation
submitted to the Department of Medicine,
the Graduate School of Yonsei University
in partial fulfillment of the requirements for the degree of
Doctor of Philosophy in Medical Science

Sang Hyun Kwak

December 2022

This certifies that the Doctoral Dissertation of
Sang Hyun Kwak is approved.

Thesis Supervisor : Sung Huhn Kim

Thesis Committee Member#1 : Jinwoong Bok

Thesis Committee Member#2 : Heon Yung Gee

Thesis Committee Member#3: Minbum Kim

Thesis Committee Member#4: Jinsei Jung

The Graduate School
Yonsei University

December 2022

ACKNOWLEDGEMENTS

I would like to express my gratitude and appreciation to all those who gave me the possibility to complete this long journey. Special thanks are due to my supervisor Prof. Sung Huhn Kim whose help, stimulating suggestions and encouragement helped me at all times of the fabrication process and in completing this doctoral dissertation. I also sincerely thank Prof. Jinwoong Bok who allowed me to be a student for a year in a basic research course in his lab and guided me in the world of basic science. I am thankful to Prof. Heon Yung Gee for providing great insight and constructive criticism of this dissertation. I sincerely appreciate Prof. Jinsei Jung, who is just like a big brother to me and a role model for physician-scientist. I thank Prof. Jae Young Choi, Prof. In Seok Moon and Prof. Minbum Kim for teaching me all about otology. It has been an honor for me to finish my resident program in the department of otorhinolaryngology at Yonsei university.

To all members of the Anatomy lab in 209 and ENT lab, I appreciate all the help you have given me. I have worked so closely and I have learned so many details of basic science. It has been an amazing experience working in the basic research lab.

I am grateful to Seong Hoon Bae, I could finish my fellowship and basic research program with you. Always grateful to Chan Min Jung, you are my best coffee mate. Also, thanks to Hyun Jin Lee and Gi Sung Nam, let us go out to play a ball.

Thanks of course to my family for their support. With their love and trust, I could finish my Ph.D. course. I give my love to my nephew Rowan, I wish for you to grow up healthy and happy. Finally, thank you, Jiweon for your constant support and love. I always love you.

<TABLE OF CONTENTS>

LIST OF FIGURES

ABSTRACT

Developmental transcriptomic profiling of non-sensory vestibular epithelium reveals ionic contribution to endolymph formation

Sang Hyun Kwak

Department of Medicine
The Graduate School, Yonsei University

(Directed by Professor Sung Huhn Kim)

In the inner ear, various ion channels have reported and play a key role in signal transduction, their malfunction could lead to hearing and vestibular dysfunction. Ion channels contribute to formation of endolymph. Endolymph is formed from embryonic day (E) 14.5 of developing murine inner ear. Endolymph secretion leads to lumen formation in developing inner ear. Although it was suggested that osmotic gradient created by changes of ionic composition plays a role in the endolymph formation, still exact molecular mechanism of endolymph formation is unknown. We aimed to investigate the mechanism of endolymph formation in the developing inner ear.

We collected non-sensory epithelium of vestibule at the age of E16.5, E18.5, and Postnatal day (P) 5, and classified the collected specimens according to the presence of dark cells as follows: non-sensory epithelium of utricle and common crus that contained dark cells and semicircular canals that did not contain dark cells. RNA sequencing was performed with those samples to analyze the changes in ion channels according to the development. After selecting candidate genes for endolymph formation, we measured endolymphatic volume changes using confocal 3D live imaging with the application of candidate ion channel inhibitors for functional study. The localization of the candidate ion channels was examined by immunohistochemistry

We selected 1613 differentially expressed genes (DEGs) by RNA sequencing analysis ($P < 0.001$ and $|\text{Fold Change}| < 2$ at least in one comparison). The genes in each sample formed close clusters according to the cell types and development period. Most

genes were related to ion activities such as ion transport, and membrane transport. Four major ions potentially involved in the endolymph formation with high probability were sodium, chloride, calcium, and potassium ions. A functional study using 3D volume change with the application of chloride-free solution and amiloride at E16.5 showed blockage of endolymphatic fluid secretion. The calcium-free solution did not show any decrease in secretion rate. Potassium ions only worked at P5, confirmed by XE991 treatment.

During inner ear development, sodium and chloride ions, but not potassium ions, are strongly associated with endolymphatic fluid secretion. These findings may help elucidate the mechanism of inner ear formation as well as congenital hearing loss and vestibular disorders.

Key words: endolymph formation, ion channel, inner ear development, RNA sequencing

Developmental transcriptomic profiling of non-sensory vestibular epithelium reveals ionic contribution to endolymph formation

Sang Hyun Kwak

Department of Medicine
The Graduate School, Yonsei University

(Directed by Professor Sung Huhn Kim)

I. INTRODUCTION

In the inner ear, various reported ion channels play a key role in signal transduction and their malfunction could lead to hearing and vestibular dysfunction. There are several cases of hereditary hearing loss related to ion channel mutation and dysfunction. Representatively, the pendrin mutation, encoded by *SLC26A4*, lead to congenital hearing loss and balance problem [1]. Meniere's disease, which may cause the alteration of fluid homeostasis of inner ear, is a typical balance disorder accompanies hearing loss and its etiologies are still unclear [2].

The inner ear comprises the cochlea, vestibule, and endolymphatic sac. The inner ear lumen is filled with endolymphatic fluid, which especially has a unique ion composition with a high potassium and a low sodium concentration [3,4]. However, the composition of perilymph, which is the fluid surrounding the endolymph membrane, is similar to other extracellular fluids that contain high sodium and low potassium ion levels. These unique ion compositions of endolymph and the proper amount of fluid volume play a key role in the sensory processing of the inner ear. High concentration of potassium results in electric current into the hair cells through mechano-sensitive channels, that depolarize hair cells. In

the vestibule, the KCNQ1 channel on dark cells on the vestibular labyrinth secrets K^+ ions into the endolymphatic lumen, similar to the KCNQ1 channel on the marginal cells at the stria vascularis of the cochlea [5-7].

The murine inner ear develops with an ectodermal invagination and forms an otocyst at the embryonic day (E) of 9.5. Initially, the otocyst is filled with plasma-like amniotic fluid. At the E 10.5, two protrusions begin to extend from the otocyst to result in the formation of the cochlea and endolymphatic sac. One protrusion elongates and coils to complete the formation of the cochlea, and the center of the otocyst becomes the vestibular labyrinth. The lumen of the endolymphatic sac opens at E11. The complete turn of the cochlea and composition of the vestibular labyrinth consisting of saccule, utricle, and ampullae are formed by E18 [8].

In the developing murine inner ear, the endolymphatic space of the cochlea begins to enlarge at the E14.5 with the secretion of fluid from the vestibular labyrinth. Without a vestibular labyrinth, the endolymphatic space of the cochlea does not open at the E14.5, however, at E17.5, the endolymphatic space of the cochlea was open without the vestibular labyrinth [9]. These results suggest that endolymphatic fluid formation begins at the vestibular labyrinth. The ionic composition of the developing inner ear is different from postnatal day [10]. In the embryonic day of mice, Na^+ ions maintain a higher concentration than K^+ ions at E16.5. On the day of E19.5, shortly before birth, the K^+ ion concentration gradually increases, which relies on the expression of the KCNQ1 channel. The K^+ ion concentration begins to rise slowly and reaches the adult levels by the third postnatal day (P). However, the factors that initiate the enlargement of endolymphatic space at the embryonic day are unclear.

Previous literature suggests that endolymphatic fluid formation begins at E14.5 with the vestibular labyrinth. The mechanism by which vestibular labyrinth secretes endolymph remains unclear. Herein, we present developmental transcriptomic profiling of non-sensory vestibular epithelium in the mice to elucidate ionic contribution to endolymph formation.

II. MATERIALS AND METHODS

1. Animal, vestibular tissue preparation and RNA isolation

C57BL/6N mice established at the National Institute on Deafness and Other Communication Disorders (NIDCD) were obtained from the Koatech, animals (Koatech, Pyeongtaek, Gyeonggi-do, Republic of Korea). The inner ears were freshly dissected from the E16.5 embryos, E18.5 and P5 mice. The vestibule is micro-dissected in a sterile normal perilymph solution (150 mM NaCl, 3.6 mM KCl, 1 mM $MgCl_2$, 0.7 mM $CaCl_2$, 10 mM HEPES, 5 mM dextrose, pH 7.4). The bony capsule was carefully removed and the whole membranous vestibular labyrinth was isolated. We separated the vestibular labyrinth into three compartments, dark cell area from the non-sensory epithelium of the utricle, common crus, and semicircular canal. The sensory epitheliums including the ampulla, utricular macula and saccular macula were excluded. Total RNAs were extracted using the RNeasy Micro Kit according to the manufacturer's protocol (Qiagen, Valencia, CA, USA). The quality of RNA was examined using Agilent Bioanalyzer (Agilent Technology, Palo Alto, CA, USA). RNA with 3` polyadenylated tails can be filtered from the isolated RNA to include only mRNA, depleted of ribosomal RNA, and attached to a substrate, typically magnetic beads. RNA was fragmented to an average length of 200 nt by magnesium-catalyzed hydrolysis and then converted into cDNA by random priming. The cDNA was converted into a molecular library for Illumina/Solexa 1G sequencing, and the resulting 25-bp reads were mapped onto the genome. All procedures involving animals were approved by the Institutional Animal Care and Use Committee at Yonsei University (IACUC#: 2020-0149).

2. RNA sequencing and bioinformatics analysis

We used CLC Genomic Workbench 9.5.3 software (Qiagen) to map the reads to the mouse genome (mm10, build name GRCm38) and generated gene expression values in the normalized form of Transcripts Per Kilobase Million values (TPKM). All differentially expressed genes (DEGs) were selected based on $p<0.01$. In addition, we conducted an RNA sequencing (RNA-seq) analysis, including hierarchical clustering and principal components analysis, using R studio v3.6.3. Functional enrichment with Gene Ontology was performed using the Database for Annotation, Visualization, and Integrated Discovery v6.8.

3. Quantitative Real-Time Polymerase Chain Reaction (qPCR)

We performed qPCR to confirm the RNA-seq data. RNA samples were purified from three biological replicates from each of the vestibular samples used for qPCR. cNDAs were synthesized from each RNA (2 μg) sample using poly $(dT)_{20}$ and the Superscript III RT kit according to the manufacturer's instructions (Invitrogen, Waltham, MA, USA). qPCR was performed for KCNE1 as dark cell marker, POU4F3 as hair cell marker, and GFAP as a neuronal marker in triplicate wells using SYBR Green PCR master Mix and the ABI 7500 RT-PCR system (Applied Biosystems, Waltham, MA, USA). The samples were denatured at 94°C for 10 minutes and then subjected to 40 cycles of denaturing at 94°C for 15 s and annealing and extension at 60°C for 1 minute. We normalized the gene expression level (ΔCt) with β-actin (*Actb*). Relative expression levels were determined by comparative methods (ΔΔCt). The primers used for qPCR were designed using the NCBI primer designing tool and are listed in Supplement Table 1.

4. In vitro measurements of fluid secretion

The membrane labyrinths of the vestibule were harvested from E16.5 and P5 and fractionated into utricles with two ampullae, common crus and semicircular canal as mentioned in the above methods. The lumens of three compartments were filled with sodium bicarbonate buffer (135 mM NaCl, 25 mM $NaHCO_3$, 4 mM KCl, 1 mM $MgCl_2$, 0.7 mM $CaCl_2$, 5 mM dextrose, pH 7.4) using manual injection system (Cell Tram vario, Eppendorf, Hamburg, Germany). Each isolated tissue is manually sealed using a fine glass needle and transferred individually to glass-bottom dishes (P35G- 1.5–10 C, MatTek, Ashland, MA, USA) filled with 200 µL DMEM, 4.5 g/L glucose, L-Glutamine and sodium pyruvate solution (Lonza) for 5 hours incubation at 37°C in 5% CO_2. We imaged the incubated tissues by three-dimensional (3D) confocal microscopy to check integrity and recovery from damage during dissection.

Eight experimental groups for every three compartments (utricle, common crus, and semicircular canal) for two different time days, E16.5 and P5 were prepared and incubated for 15 to 24 hours in an incubation chamber at 37°C with 5% CO_2.

For all experiments, incubated tissues were imaged by 3D confocal microscopy. Imaging consisted of scanning microscopy and superimposition of transmission images recorded with red (633 nm), green (561 nm) and blue (405 or 458 nm) lasers (20x/0.8 objective; custom hardware configuration of LSM 780, Carl Zeiss, Jena, Germany). Using Zen black (Carl Zeiss, Jena, Germany), surface areas of the utricle, common crus, and semicircular canal, were obtained and geometrically calculated by following the formula presented in Figure 1. For geometric simplification, the luminal volume of the ampulla was modeled as a round sphere and the utricle as a spheroid. The luminal volume of the common

crus and semicircular canal were geometrically simplified as a cylinder. Fluid secretion rates were presented as nL x hr^{-1} x mm^{-2}.

5. Solutions and pharmacological agents

Immediate after 5 hours of incubation, we changed the incubation solutions to seven solutions and chemicals. After DMEM was removed from the incubation dish, we changed the incubation solution to sodium bicarbonate buffer, in the first group as a control. Based on RNA-seq data, we changed the DMEM solution to several pharmacological agents. We prepared 100 μM amiloride (A7410, Sigma-Aldrich, St. Louis, MO, USA) for blocking ENaC and 1 μM cariporide (SML1360, Sigma-Aldrich, St. Louis, MO, USA) for NHE1 to determine the relevance of sodium ion. 100 μM of XE991 (X2254, Sigma-Aldrich , St. Louis, MO, USA) was used to block the KCNQ1. 100 μM of ouabain (O3125, Sigma-Aldrich , St. Louis, MO, USA) as an NA^+/K^+ ATPase inhibitor and bumetanide (B3023, Sigma-Aldrich , St. Louis, MO, USA) as an $NA^+/K^+/Cl^-$ inhibitor were also treated. No specific chloride ion channel blockers are available; hence, we used chloride-free solutions (150 mM Na-gluconate, 1.6 mM K_2HPO_4, 0.4 mM KH_2PO_4, 1 mM $MgCl_2$, 4 mM Ca-gluconate, 5 mM dextrose, pH 7.4).

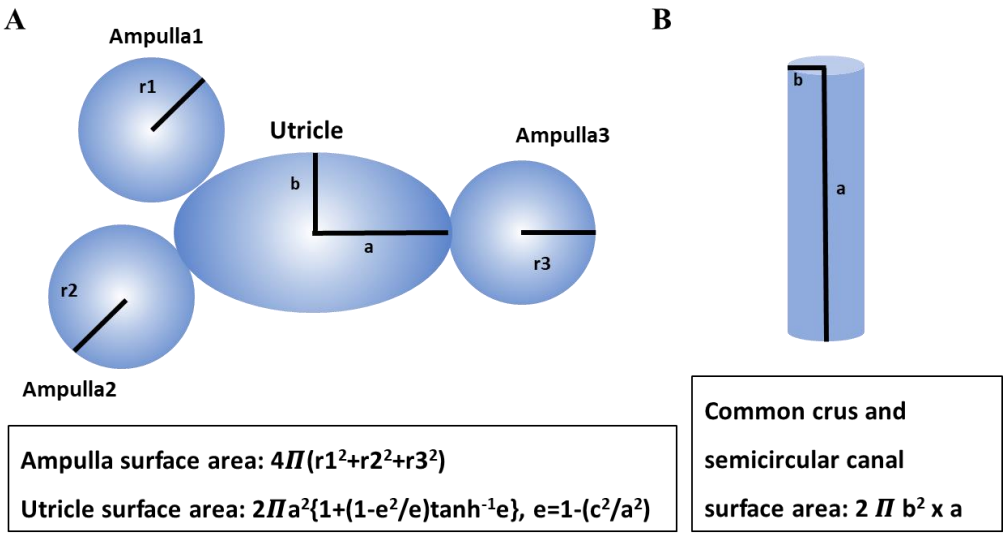

Figure 1. Luminal volumes of the utricle, common crus and semicircular canal were calculated through geometrical simplification. (A) Utricular volume was calculated as a spheroid and ampulla volume as a sphere. (B) Common crus and semicircular canal volumes were calculated as a cylinder.

6. Cryosection and Immunohistochemistry

For histological analysis, cryosection was performed. E16.5 embryos and P5 mice pup were fixed in 4% paraformaldehyde for two days, mounted in OCT compound (Tissue-Tek, Tokyo, Japan) and sectioned at a thickness of 12 μm onto Superfrost Plus slides (Tissue-Tek, Tokyo, Japan) using a cryostat (Thermo Fisher Scientific, Waltham, MA, USA).

For the immunohistochemistry of KCNE1, KCNQ1, and ENaC, frozen sectioned inner ear tissues of E16.5 and P5 were used. Immunofluorescent staining was performed as previously described [11]. The following antibodies were used; KCNE1 rabbit, polyclonal antibody (1:200, Product # APC-163, Alomone labs, Jerusalem, Israel), KCNQ1 mouse monoclonal antibody (1:100, Product # sc-365186. Santa Cruz, Dallas, TX, USA), and Alpha-ENaC Rabbit Polyclonal antibody (1:200, Product #PA1-920A, Thermo Fisher Scientific, Waltham, MA, USA). Secondary antibodies used were Alexa Fluor 568, and 647 antibodies (1:1000, Themo Fisher Scientific , Waltham, MA, USA).

7. Statistical analysis

We performed the Kruskal-Wallis H test and post-hoc Dunn's multiple comparisons test for the comparison of multiple groups. All graphs visualized the mean and SEM values. Prism 8.0 (GraphPad Software, San Diego, CA, USA) software was used for the statistical analyses. $P < 0.05$ were considered statistically significant.

III. RESULTS

1. Developmental transcriptomic analysis reveals ion transport related to endolymphatic formation in mice.

We performed RNA-seq in E16.5, and E18.5 embryos and P5 mice to investigate fluid secretion for endolymphatic lumen formation in the vestibule. Principal component analysis (PCA) plot for RNA-seq data of utricle, common crus, and semicircular canals isolated at E16.5, E18.5 and P5 is shown in Figure 2A. A total of 1,613 differentially expressed genes (DEGs) were selected [$P < 0.001$ (t-test) and |fold change| >2 at least in one comparison] and used for PCA. The RNA-seq results of nine samples clustered are in order of two directions, which are developing time and tissue difference. PCA plot showed sequential development from E16.5 to P5. Non-sensory epithelium of the utricle contains dark cells, and common crus only include dark cells on one side. Whereas semicircular canals do not contain any dark cells. These differences appeared on the PCA plot. The red series shows the non-sensory epithelium of the utricle. The yellow series show common crus, and the blue series shows a semicircular canal.

To identify functional pathways associated with expressed genes from nine samples, we performed gene ontology (GO) enrichment analysis. Heatmaps from clustering analysis of 1613 DEGs showed three patterns (Figure 2B). We divided it into three clusters, firstly, we divided one cluster into the increased pattern of gene expression gradually through developmental time. Second clusters are defined as the decreased gene expression pattern through time. The third cluster is defined as increased gene expression in order of utricle, common crus, and semicircular canal, which is the amount of dark cell area. The most expressed gene function was the regulation of ion transmembrane transport in cluster one and cluster two. Interestingly, GO analysis of cluster three revealed gene function related to sensory perception and ear development (Figure 2C).

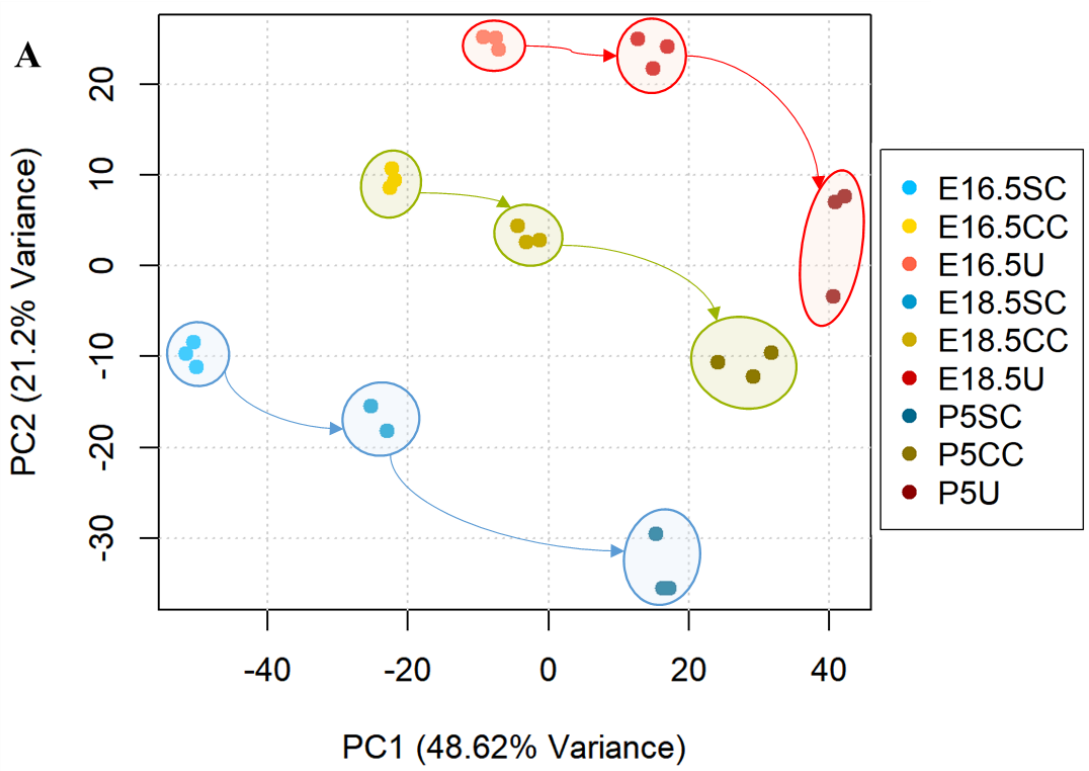

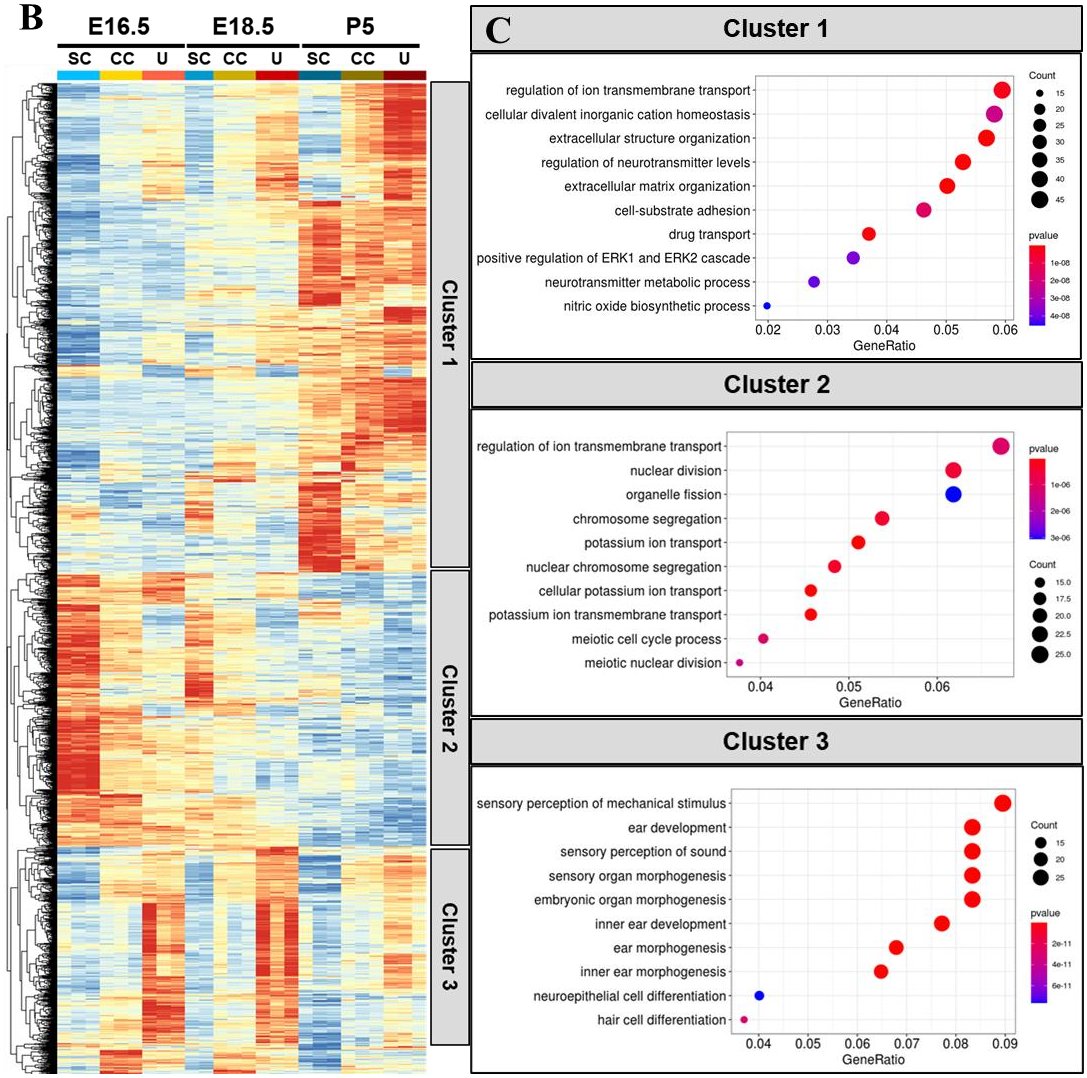

Figure 2. RNA sequencing reveals changes in genes related to ion transport during the development of vestibule in mice. (A) Principal component analysis (PCA) plot for RNA sequencing data of semicircular canals, common crus, and utricle isolated at E16.5, E18.5, and P5. A total of 1,613 differentially expressed genes (DEGs) were selected [$P < 0.001$ (t-test) and |Fold Change| > 2 at least in one comparison] and used for PCA. (B) Heatmaps

from clustering analysis (Euclidean, complete linkage) of 1,613 DEGs. Two heatmaps show clustering patterns in longitudinal (left) and topological (right) arrangement among samples, (C) Gene Ontology (GO) analysis of 1,613 DEGs. GO enrichment was retrieved using DAVID and 11 GO terms related to ion transport in the molecular function category were plotted against –log (P value). Bars of GO terms associated with potassium (red), sodium (orange), chloride (green), and calcium (blue) are indicated with different colors.

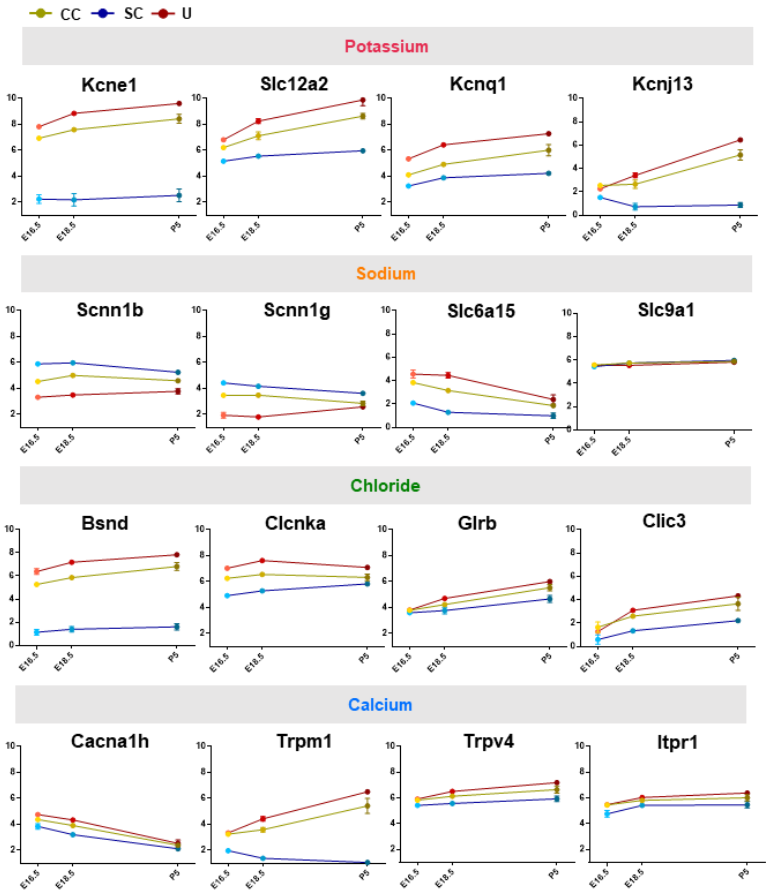

Figure 3. Representative genes of ion channels from RNA sequencing. Graphs showing expression pattern of four representative genes that directly transport potassium, sodium, chloride and calcium ion.

Since the dark cell including KCNQ1 channels has been implicated in fluid secretion during postnatal, we identified specific ion-related genes like potassium, sodium, chloride, and calcium (Figure 3). Representative genes associated with potassium ions were *Kcne1* and *Kcnq1*, which expression level was gradually increased through time and high in utricle. The subunit genes consisting of the Epithelial sodium channel (ENaC) were representative genes of sodium ions. *Scnn1b* and *Scnn1g* were mostly expressed in the semicircular canal. *Slc9a1* expressed highly from E16.5 to P5. *Bsnd* and *Clcnka* were representative genes related to chloride ions and their expression level was high in utricle. In association with calcium ion, *Cacna1h*, *Trpm1* and *Trpv4* were expressed.

2. In vitro fluid secretion measurement showed importance of Na^+ and Cl^- ion in inner ear development.

Based on RNA-seq data, we dissected the utricle and ampulla, common crus and semicircular canal and sealed them to create a closed cavity at E16.5 and P5. The sealed tissues were incubated at DMEM for five hours in an incubation chamber at 37°C with 5 % CO_2. Under the confocal microscope, we checked healthy and well-swollen tissues and obtained initial volume and luminal surface area. We selected specific ion channel blockers to clarify the ion channel responsible for the fluid secretion and incubated them for 10–20 hours in a chamber. We calculated and quantified the fluid secretion rate presented as nl x hr^{-1} x mm^{-2}. Eight pharmacological experiments were performed.

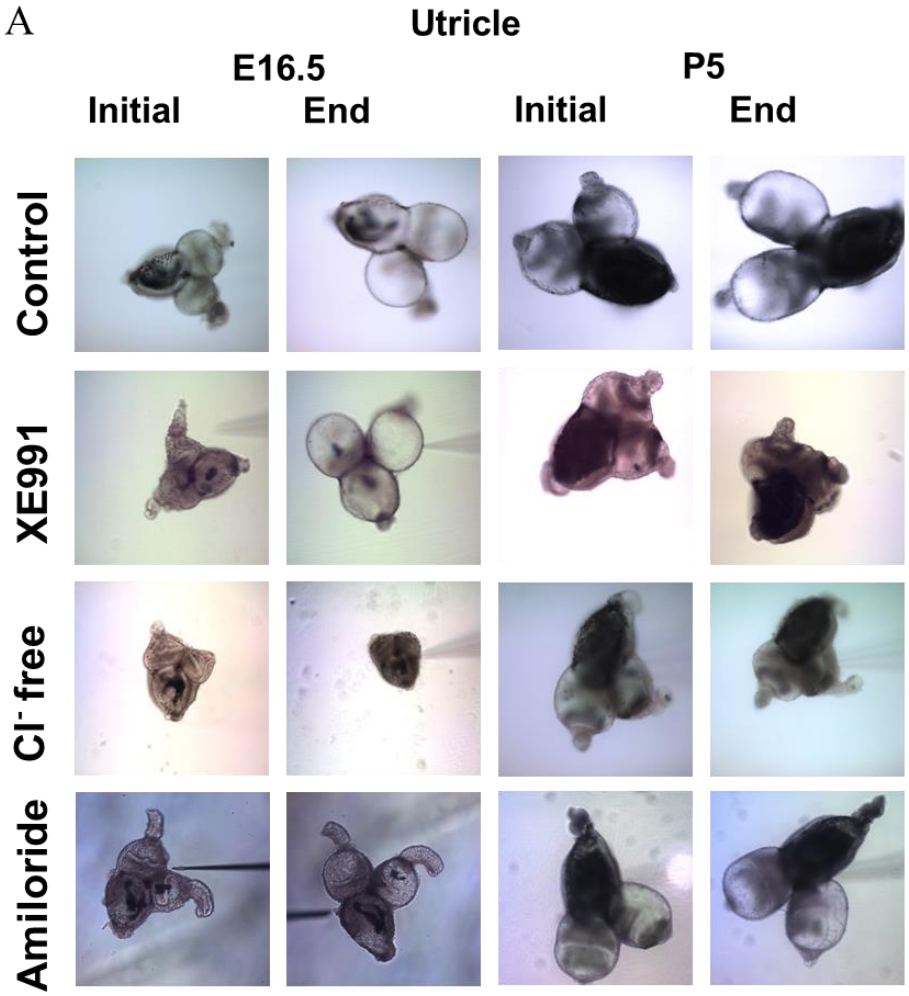

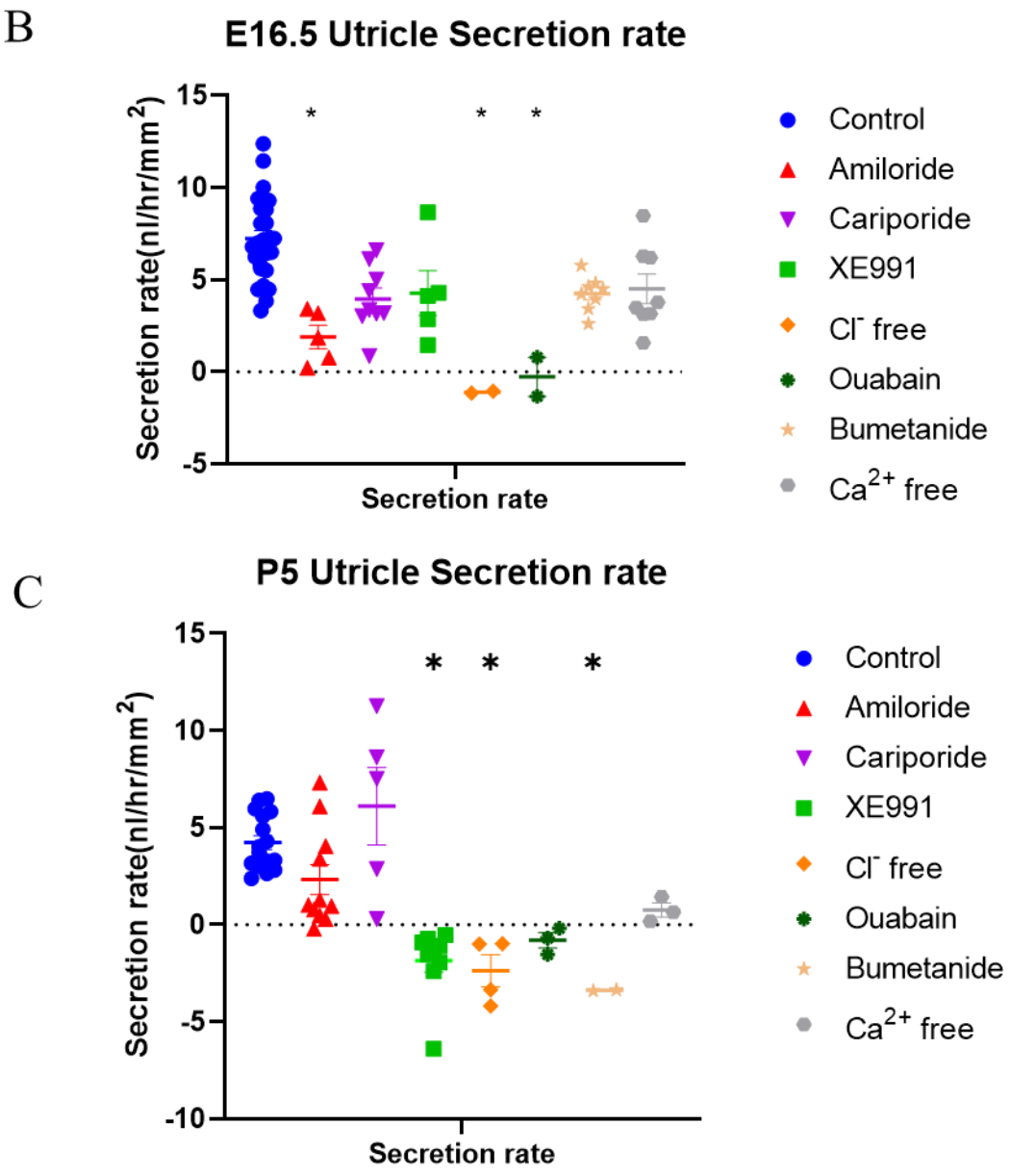

Figure 4. Endolymphatic fluid secretion and pharmacological treatment in utricle at E16.5 and P5. (A) Representative image of the utricle and two ampullae. Confocal microscopic images were taken before pharmacological treatment and broadly 20 hours of

incubation. (B) Amiloride, Cl^- free solution, Ouabain showed a significantly lower secretion rate at E16.5 ($P < 0.05$). (C) XE991, Cl^- free solution, and bumetanide treatment showed lower secretion rate at P5 ($P < 0.05$).

In the first group of experiments, the utricle and ampulla showed a significant increase in volume at E16.5 and P5 in the control, sodium bicarbonate buffer (Figure 4A-C). Amiloride, an ENaC blocker, showed a significant decrease in secretion rate at E16.5 not at P5. XE991, a KCNQ blocker showed a reduced secretion rate at P5, in contrast to E16.5. Cariporide, which is an NHE channel blocker, did not show any difference compared with the control group, at both E16.5 and P5. In relation to chloride ions, a chloride ion-free solution was used to incubate the experimental groups. Both E16.5 and P5 utricles were reduced significantly compared with the control group. The dark cell and stria vascularis, Na-K-Cl (NKCC) cotransporter and Na-K-ATPase are present at a basal area [12]. To confirm those channels, we experimented with NKCC inhibitor, bumetanide, and Na-K-ATPase inhibitor, ouabain. At E16.5, the ouabain experimented group showed a significantly decreased secretion rate, whereas at P5, did not show any difference. Bumetanide showed decreased secretion rate only at P5. The Ca-free solution did not show any decreased secretion rate in both E16.5 and P5.

In the second experimental group, the common crus was sealed at both ends and incubated. One side of the common crus contains a dark cell, the other lumen is the same membrane as the semicircular canal. Compared to the control group, chloride-free solution, ouabain and bumetanide showed significantly lower secretion rates at E16.5 (Figure 5A-B). Amiloride did not show any statistically significant decrease in secretion rate at E16.5. At P5, XE991 and chloride-free solution showed a statistically significant reduction of secretion rate (Figure 5A, 5C).

In the third experimental group, the semicircular canal was sealed at both ends and incubated. At E16.5, amiloride, XE991, chloride-free solution, and bumetanide were significantly lower, compared to the control group (Figure 6A-B). At P5, all experimental groups did not show any statistical differences (Figure 6C).

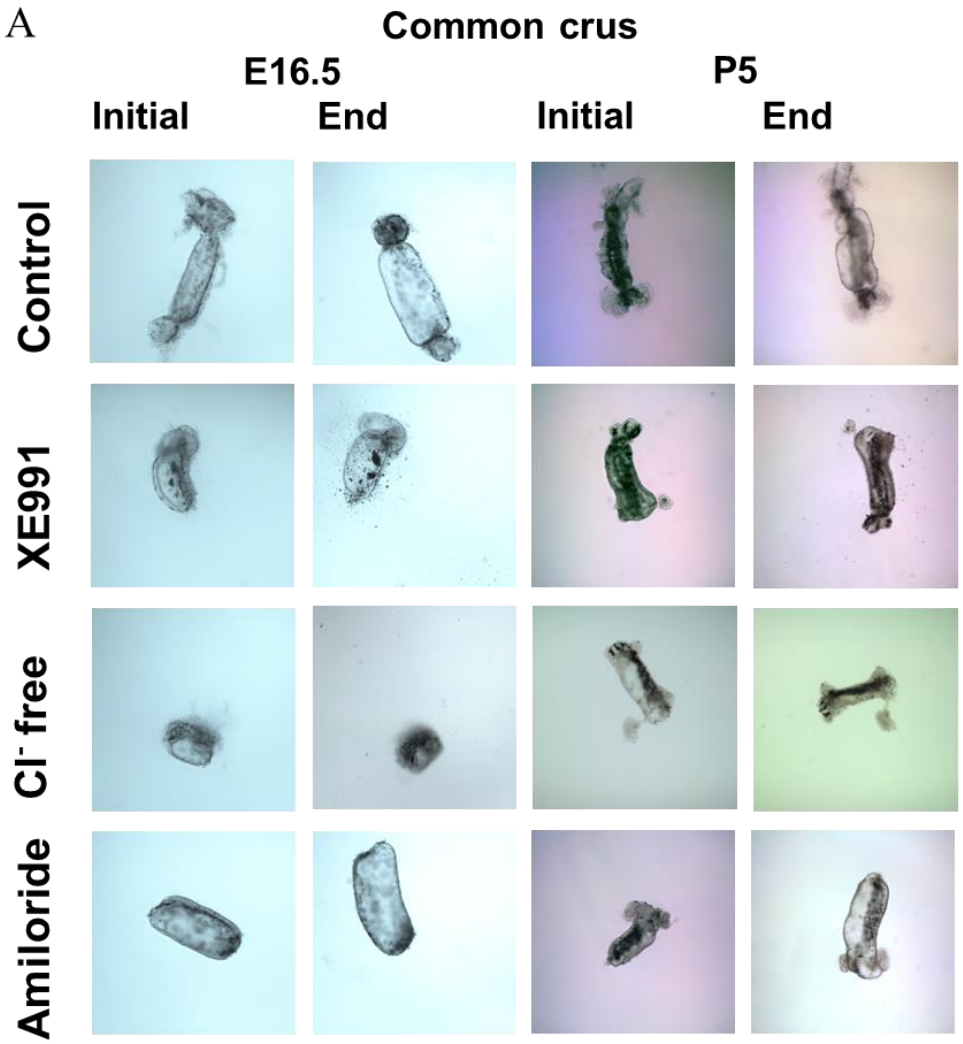

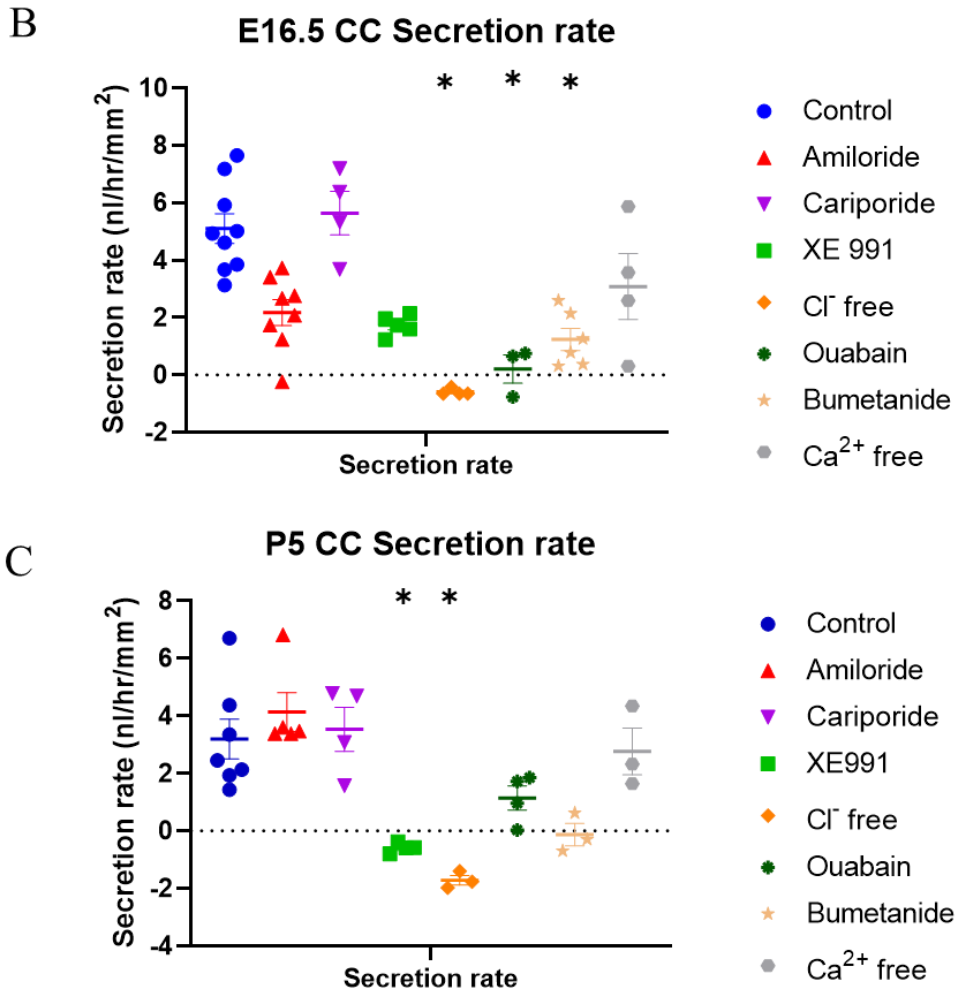

Figure 5. Endolymphatic fluid secretion and pharmacological treatment in Common crus at E16.5 and P5. (A) Representative image of common crus. Confocal microscopic images were taken before pharmacological treatment and broadly 20 hours of incubation. (B) Cl^- free solution, ouabain and bumetanide showed significantly lower secretion rates than the control at E16.5 ($P < 0.05$). (C) XE991 and Cl^- free solution treatment showed a lower secretion rate than the control at P5 ($P < 0.05$).

A

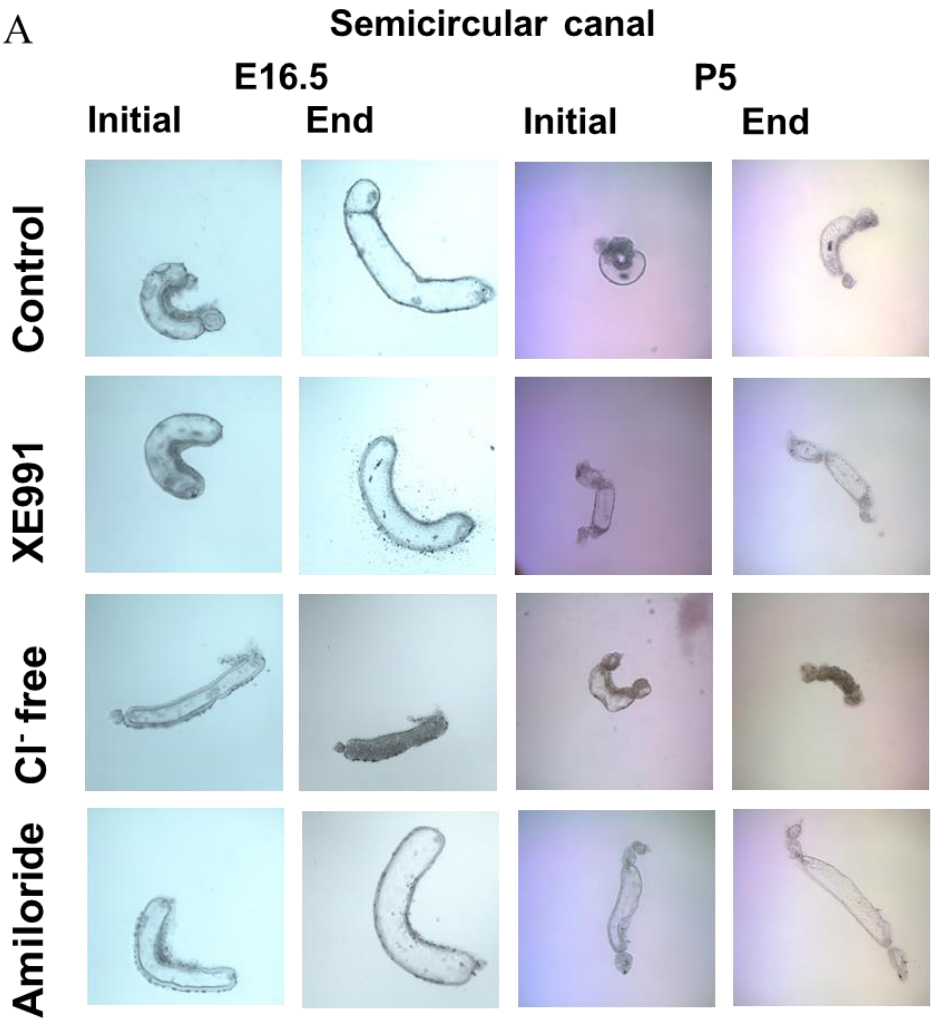

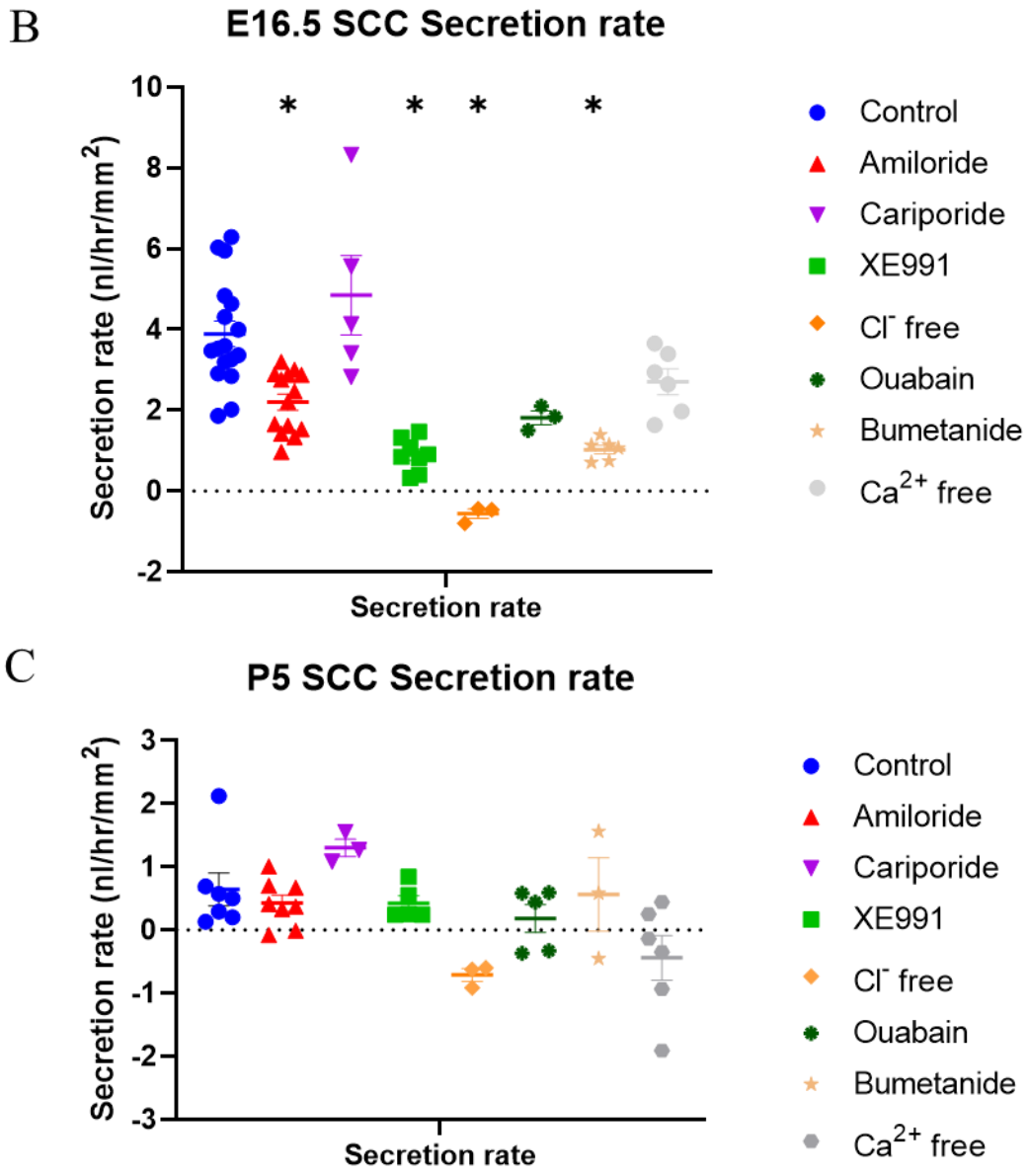

Figure 6. Endolymphatic fluid secretion and pharmacological treatment in the semicircular canal at E16.5 and P5. (A) Representative image of the semicircular canal. Confocal microscopic images were taken before pharmacological treatment and broadly 20

hours of incubation. (B) Amiloride, XE991, Cl^- free solution, and bumetanide showed significantly lower secretion rates at E16.5 ($P < 0.05$). (C) There was no difference in secretion rate among the eight experimental groups at P5.

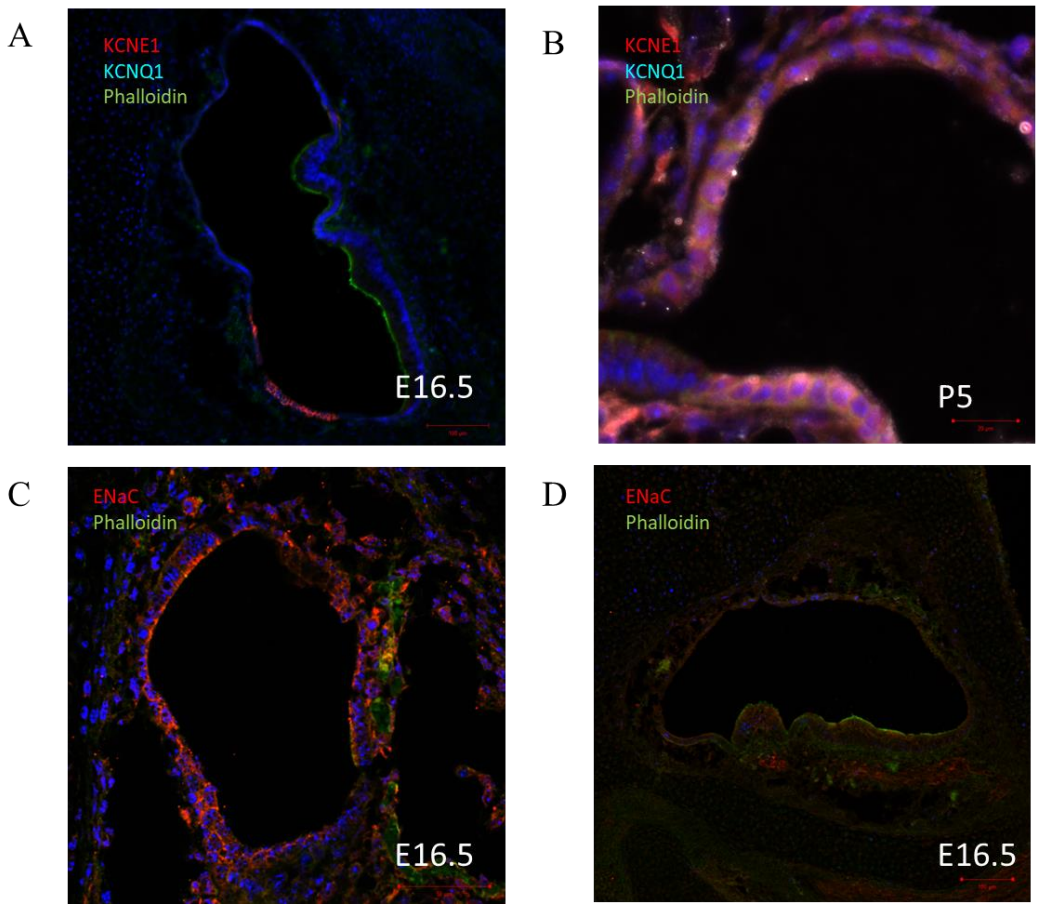

Figure 7. Localization of KCNE1, KCNQ1 and ENaC in vestibule at E16.5 and P5. (A) KCNE1 (red) was expressed at the non-sensory epithelium of the utricle at E16.5, whereas KCNQ1 (cyan) did not express. (B) KCNE1 and KCNQ1 co-expressed at the same location, apical membrane of the non-sensory epithelium of the utricle and base of the ampulla. (C) ENaC (red) is expressed at the apical membrane of the semicircular canal. (D) ENaC is located at the non-sensory epithelium of the utricle at E16.5.

3. KCNE1 and ENaC located apical membrane of the non-sensory epithelium of vestibule at E16.5 and KCNQ1 at P5.

Expression of KCNE1 was detected by immunohistochemistry in the apical membranes of dark cells in the non-sensory epithelium of the utricle at E16.5 (Figure 7A), whereas KCNQ1 was not detected. At P5, both KCNE1 and KCNQ1 were detected in the same location on the apical membrane of the non-sensory epithelium of the utricle and base of crista ampullaris (Figure 7B). ENaC was detected in the apical membrane of the semicircular canal at E16.5 (Figure 7C). There was a broad expression at the non-sensory epithelium of the utricle at E16.5 (Figure 7D).

IV. DISCUSSION

Our study provides a clue to elucidate endolymphatic fluid secretion in the developing inner ear. Based on RNA-seq data, the non-sensory epithelium of the vestibule mostly contains various ion channels. We confirmed potassium-induced endolymphatic fluid formation at P5 (Figure 4). The gene expression values of *Kcnq1* and *Kcne1* gradually increased from E16.5 to P5 (Figure 3). At the E16.5, *Kcnq1* expression was not revealed by immunohistochemistry (Figure 6A). A few samples expressed KCNE1 at the non-sensory epithelium of the utricle. According to the functional study, XE991 treatment at P5 showed decreased luminal volume and secretion rate (Figure 4). In addition, the ionic composition of the endolymph at E16.5 showed a high sodium concentration [10].

The human inner ear reaches maturity earlier than that of the mouse, before birth. Vestibular reflexes are first elicited at 19 weeks gestation. In addition, type II vestibular hair cell produces voltage current at 12 weeks gestation. In the human cochlea, by 20–22 weeks gestation, scala media reaches maturity, hence, the auditory startle reflex is first elicited at 24 weeks gestation [13]. We mentioned above that endolymph formation is necessary for mechano-sensory production. The secretion of endolymph fluid in human development is much earlier than in the mouse. This is consistent with our data, *kcne1* and *kcnq1* expression gradually increased from E16.5 and P5. In addition, the functional study of XE991 showed the function of KCNQ1 channels at P5, not E16.5 (Figure 4).

Next, we experimented with the relevance of calcium ions. The *Cacna1h* showed a gradually decreased TPKM from E16.5 to P5. (Figure 3). *Cacna1h* encodes a T-type calcium channel, CACNA1H, which is important for calcium influx and depolarization of cells [14]. In the inner ear, CACNA1H is physiologically important for auditory information processing in adult mice [15]. In the functional study, we considered calcium deprivation may lead to cell death. Calcium-free solution, which excludes calcium chelating agent, ethylene-diamine-tetraacetic acid, was used to determine the relevance of calcium ions. The secretion rate of the calcium-free solution did not show any difference

at any time, and Mibefradil, which is a CACNA1H blocker and does not show in the functional study. Thus, we ruled out calcium ions with respect to endolymph formation.

According to RNA-seq data, various chloride ion channels were identified, including BSND. *Bsnd* encodes barttin, a β-subunit of the CLC-Ka chloride channel. BSND is located at the basal membrane of marginal cells in stria vascularis and dark cells in the vestibule [16]. Since BSND is not located at the apical membrane, it is not responsible for endolymph formation. Unexpectedly, the secretion rate of chloride-free solution decreased significantly at both E16.5 and P5 (Figure 4–6). At P5, chloride ions are essential for potassium secretion via the CLC-Ka channel. However, chloride-free solution treatment showed decreased secretion rate at E16.5, indicating that chloride ions are essential to the formation of endolymph at the development stage. Interestingly, increased chloride ion concentration in the lumen creates an electrochemical gradient for Na movement across the cell junction in the sweat secretion system [17]. We identified no specific chloride ion channel blocker relation with RNA-seq data to substantiate specific ion channels. This was a limitation of our study.

We further investigated the relevance of sodium ion, which is highly concentrated in endolymph at the developmental stage. In the basolateral membrane of dark cells, Na^+/H^+ exchanger NHE-1 is present [18]. Likewise, *Slc9a1*, which encodes NHE-1, was expressed highly regardless of developmental stage. We used an NHE blocker, cariporide in the functional study. However, the secretion rate did not show any difference in all tissues at both E16.5 and P5. *Scnn1b*, which encodes ENaC β subunit, was mostly expressed in the semicircular canal than the utricle. We used amiloride to block the ENaC channel. At a high micromolar concentration of 100 μM, amiloride treated utricle and semicircular canal showed decreased secretion rate at only E16.5. The results need to be interpreted cautiously, because a high dose of amiloride may also block other membrane transport pathways including Na^+/H^+ exchanger [19]. In addition, evidence suggests additional amiloride-sensitive channels in non-sensory cells of the saccule, where ENaC is located [20]. In the kidney and the sweat glands, ENaC absorbs sodium into the cell from the lumen [21,22].

In conclusion, sodium transport into the endolymphatic space may play a significant role in the endolymph formation, however, we could not confirm specific ion channels in the apical membrane, such as ENaC and NHE1 (Figure 8).

Potassium ions do not play a key role in endolymphatic fluid formation in the developing inner ear (Figure 8). Chloride and sodium ions contribute to endolymph formation at E16.5. NKCC expressed at E18.5 in the cochlea at the basolateral membrane of the dark cell, which explains why bumetanide did not work at E16.5 in the utricle [23]. The result of XE991 and bumetanide in the common crus and semicircular canal at E16.5 might have been due to the technical issues of incubation. NaK-ATPase also contributes to endolymph formation at both times E16.5 and P5. However, it is located at the basolateral membrane. Further research is required to identify specific ion channels located at the apical membrane of the dark cell. Further study, such as an electrophysiological experiment is needed to clarify the result of the functional study.

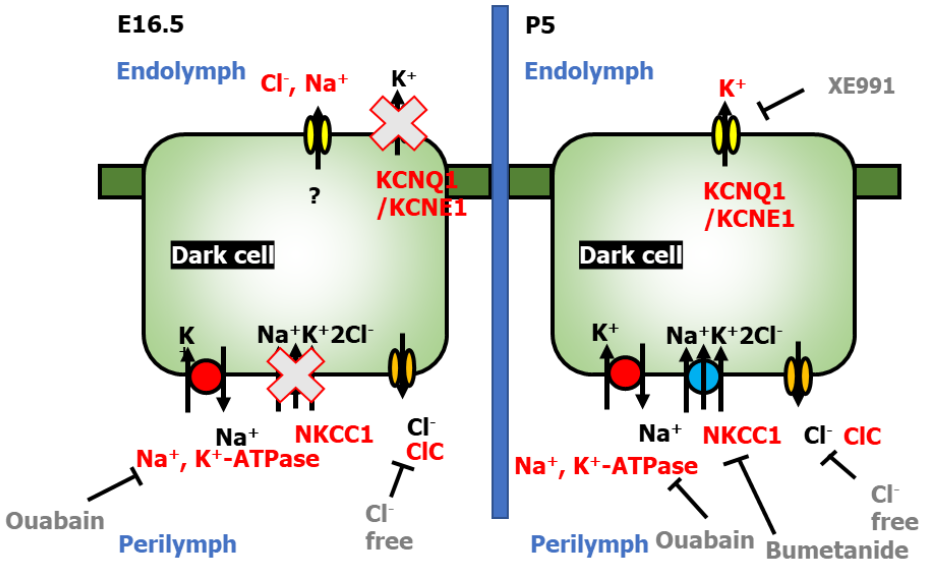

Figure 8. Diagram of ion transport in the dark cell at E16.5 and P5. The sodium and chloride ions play a key role in endolymphatic fluid formation at E16.5. NaK-ATPase and CLC-K at the basolateral membrane are important ion channels both at E16.5 and P5. Potassium ion is responsible for endolymph formation at postnatal.

V. CONCLUSION

During inner ear development, chloride and sodium ions, but not potassium ions, are strongly associated with endolymphatic fluid formation. This finding may contribute to elucidating inner ear development and the origin of endolymph as well as hearing loss and vestibular disorders such as Meniere's disease.

.

REFERENCES

1. Dror AA, Brownstein Z, Avraham KB. Integration of human and mouse genetics reveals pendrin function in hearing and deafness. Cell Physiol Biochem. 2011;28(3):535-44.
2. Rizk HG, Mehta NK, Qureshi U, Yuen E, Zhang K, Nkrumah Y, et al. Pathogenesis and Etiology of Meniere Disease: A Scoping Review of a Century of Evidence. JAMA Otolaryngol Head Neck Surg. 2022 Apr 1;148(4):360-8.
3. Smith CA, Lowry OH, Wu ML. The electrolytes of the labyrinthine fluids. Laryngoscope. 1954 Mar;64(3):141-53.
4. Sellick PM, Johnstone BM. Production and role of inner ear fluid. Prog Neurobiol. 1975;5(4):337-62.
5. Wangemann P, Marcus DC. K(+)-induced swelling of vestibular dark cells is dependent on Na+ and Cl- and inhibited by piretanide. Pflugers Arch. 1990 May;416(3):262-9.
6. Wangemann P, Liu J, Shiga N. The pH-sensitivity of transepithelial K+ transport in vestibular dark cells. J Membr Biol. 1995 Oct;147(3):255-62.
7. Wangemann P, Shen Z, Liu J. K(+)-induced stimulation of K+ secretion involves activation of the IsK channel in vestibular dark cells. Hear Res. 1996 Oct;100(1-2):201-10.
8. Wangemann P. The role of pendrin in the development of the murine inner ear. Cell Physiol Biochem. 2011;28(3):527-34.
9. Kim HM, Wangemann P. Failure of fluid absorption in the endolymphatic sac initiates cochlear enlargement that leads to deafness in mice lacking pendrin expression. PLoS One. 2010 Nov 17;5(11):e14041.
10. Li X, Zhou F, Marcus DC, Wangemann P. Endolymphatic Na(+) and K(+) concentrations during cochlear growth and enlargement in mice lacking Slc26a4/pendrin. PLoS One. 2013;8(5):e65977.
11. Jeong J, Kim JY, Hong H, Wangemann P, Marcus DC, Jung J, et al. P2RX2 and P2RX4 receptors mediate cation absorption in transitional cells and supporting cells of the utricular macula. Hear Res. 2020 Feb;386:107860.
12. Bartolami S, Gaboyard S, Quentin J, Travo C, Cavalier M, Barhanin J, et al. Critical roles of transitional cells and Na/K-ATPase in the formation of vestibular endolymph. J Neurosci. 2011 Nov 16;31(46):16541-9.
13. Lim R, Brichta AM. Anatomical and physiological development of the human inner ear. Hear Res. 2016 Aug;338:9-21.
14. Algahtani HA, Shirah BH, Samman A, Alhazmi A. Epilepsy and Hearing Loss in a Patient with a Rare Heterozygous Variant in the CACNA1H Gene. J Epilepsy Res. 2022 Jun;12(1):33-5.
15. Lundt A, Seidel R, Soos J, Henseler C, Muller R, Bakki M, et al. Cav3.2 T-Type Calcium Channels Are Physiologically Mandatory for the Auditory System. Neuroscience. 2019 Jun 15;409:81-100.
16. Rickheit G, Maier H, Strenzke N, Andreescu CE, De Zeeuw CI, Muenscher A, et al. Endocochlear potential depends on Cl- channels: mechanism underlying deafness in Bartter syndrome IV. EMBO J. 2008 Nov 5;27(21):2907-17.
17. Baker LB. Physiology of sweat gland function: The roles of sweating and sweat composition in human health. Temperature (Austin). 2019;6(3):211-59.
18. Wangemann P, Liu J, Shiga N. Vestibular dark cells contain the Na+/H+ exchanger NHE-1 in the basolateral membrane. Hear Res. 1996 May;94(1-2):94-106.
19. Kleyman TR, Cragoe EJ, Jr. Amiloride and its analogs as tools in the study of ion transport.

J Membr Biol. 1988 Oct;105(1):1-21.
20. Kim SH, Marcus DC. Endolymphatic sodium homeostasis by extramacular epithelium of the saccule. J Neurosci. 2009 Dec 16;29(50):15851-8.
21. Hamm LL, Feng Z, Hering-Smith KS. Regulation of sodium transport by ENaC in the kidney. Curr Opin Nephrol Hypertens. 2010 Jan;19(1):98-105.
22. Quinton PM. Cystic fibrosis: lessons from the sweat gland. Physiology (Bethesda). 2007 Jun;22:212-25.
23. Abbas L, Whitfield TT. Nkcc1 (Slc12a2) is required for the regulation of endolymph volume in the otic vesicle and swim bladder volume in the zebrafish larva. Development. 2009 Aug;136(16):2837-48.

APPENDICES

Supplement table 1.

PCR primer	**Sequence (5' to 3')**
Kcne1 F	CGA CTG TTC TGC CCT TTC TG
Kcne1 R	CTC AGT GGT GCC CCT ACA AT
Kcnq1 F	CTG TAC ATT GGC TTT CTG GGC CTT ATC T
Kcnq1 R	TTT TCT GAG ATG GGG ATG AAC AAA GAT G
Pou4f3_F	CGA CTT ACT TGA GCA CAT CTC G
Pou4f3_R	TTA GGC TCT CCA GGC TCC TC
Gfap F	GCA CTC AAT ACG AGG CAG TG
Gfap R	GGC GAT AGT CGT TAG CTT CG

ABSTRACT(IN KOREAN)

비감각 전정 상피의 발달 전사체 프로파일링을 통한 내림프 형성에 대한 이온 기여 규명.

<지도교수 김성헌>

연세대학교 대학원 의학과

곽상현

내이에서 다양한 이온 채널이 보고되었으며, 이들은 신호전달에서 핵심적인 역할을 하며, 이온 채널의 오작동은 청력 및 전정 기능 장애로 이어질 수 있다. 이온 채널은 내림프 형성에 기여하고 있다고 알려져 있다. 내림프는 쥐의 내이 발달 시기인 E14.5 에서 형성 된다. 내림프 분비는 내이 발달에서 곧, 내강의 형성으로 이어진다. 이온 조성의 변화에 의해 생성되는 삼투압 구배가 내림프 형성에 역할을 한다고 제안되었지만, 내림프 형성의 분자적 매커니즘에 대해 알려진 바는 없다. 우리는 발달 중인 내이에서 내림프 형성의 매커니즘을 밝히고자 하였다.

E16.5, E18.5 그리고 P5 시기의 비감각 전정 상피를 채취하여, 어둠 세포의 존재 여부에 따라 분리하여, RNA 시퀀싱을 수행하였다. 이들 조직들은 난형낭의 비감각 상피, 공통 각, 세반고리관으로 나누어 분석하였다. RNA 시퀀싱 결과를 바탕으로 하여, 내림프 형성에 기여를 할 것이라고 생각되는 각 이온 채널의 억제제를 이용하여 인큐베이션 실험을 진행하였다. 공초점 3D 이미징을 사용하여, 내림프 용적 변화를 측정하였고, 면역조직화학법으로 후보 이온 채널의 위치를 조사하였다.

총 1613개의 차별적으로 발현된 유전자 (DEG)가 RNA 시퀀싱 결과에 의해 선택되었다. 각 샘플의 유전자는 세포 유형 및 발달 기간에 따라 밀접한 클러스터를 형성하였따. 대부분의 유전자는 이온 수송, 막

수송과 같은 이온 활동과 관련이 있었다. 나트륨, 염화 이온, 칼슘 및 칼륨 이온과 관련하여 인큐베이션 및 화학적 처치 실험을 진행하였다. E16.5에서 나트륨과 염화 이온과 관련된 내림프 형성 실험에서 의미 있는 결과를 얻을 수 있었다. P5에서는 이미 알려진 대로 칼륨 이온 채널 억제제인 XE991을 통하여 내림프 형성이 저해되는 것을 확인 할 수 있었다.
내이 발달 과정에서는 태생이후와는 다르게 칼륨 이온 채널의 발현이 늦어짐으로 인하여 칼륨 이온이 내림프 형성에 관여하지 않는다. 나트륨 및 염화 이온이 내림프액 형성과 관련하여 중요한 역할을 한다고 생각된다.

핵심되는 말 : 내림프 형성, 이온 채널, 내이 발달, RNA 시퀀싱

PUBLICATION LIST

Kwak SH, Kim MK, Kim SH, Jung J. Audiological and Vestibular Functions in Patients With Lateral Semicircular Canal Dysplasia and Aplasia. Clin Exp Otorhinolaryngol. 2020 Aug;13(3):255-60

Kwak SH, Moon YM, Nam GS, Bae SH,Kim SH, Jinsei Jung, Choi JY. Clinical experience of vibroplasty with direct coupling to the oval window without use of a coupler. The Laryngoscope. 2020.130(12);E926-E932